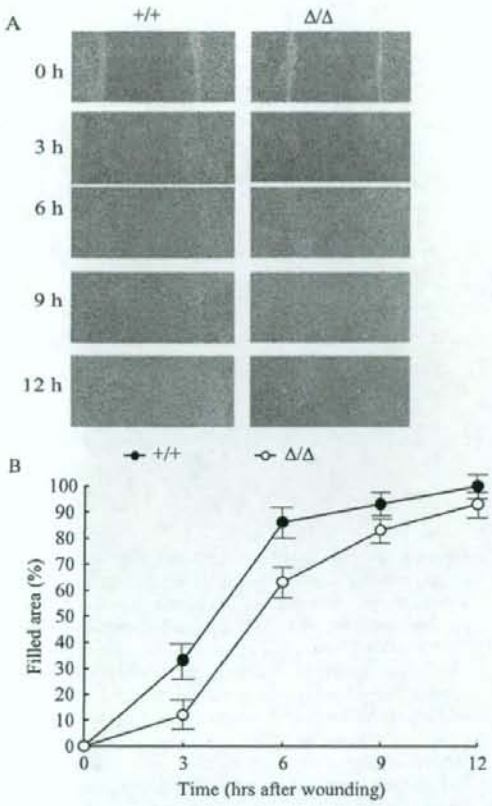

Figure 2 Delayed migration of Cas exon $2^{\Delta/\Delta}$ cells in the initial phase in the wound healing assay. (A) Photographs of Cas exon $2^{+/+}$ cells and Cas exon $2^{\Delta/\Delta}$ cells at 0, 3, 6, 9 and 12 h after wounding. Cells were first grown to confluence in plastic culture dishes, and a wound was made in the cell monolayer using a sterile micropipette tip. Cell movement was assessed 0, 3, 6, 9 and 12 h after wounding. Photographs were taken under a microscope with an objective of 100×. (B) The percentage of reduced distance between the nuclei of cells at each time period relative to the distance between two rims in the cleared field at the beginning was taken as the index (*error bars* show the standard deviation). Results presented here are representative mean values of three independent experiments.

we first performed wound healing cell migration assays. Migratory processes were assessed at 0, 3, 6, 9 and 12 h after wounding (Fig. 2A). Mean percentages of the filled area at each time points are shown in Fig. 2B. Three hours after wounding, Cas exon $2^{+/+}$ cells had filled over 30% of the gap and the cells migrating from both ends of the wound had achieved cell–cell contact. In contrast, only 10% of the area was filled by Cas exon $2^{\Delta/\Delta}$ cells. After 6 and 9 h, the migration deficit in Cas exon $2^{\Delta/\Delta}$ cells was less apparent but still present, and at 12 h the gap was almost filled in both types of the cells. This result demonstrated that Cas exon $2^{\Delta/\Delta}$ cells were deficient in ability to migrate, especially in the early phase of the response.

Cas exon $2^{\Delta/\Delta}$ cells show reduced spreading activity on fibronectin (FN)

We next examined the roles of Cas exon 2 in cell attachment, cell adhesion and cell spreading on FN. The morphological changes in Cas exon $2^{+/+}$ and Cas exon $2^{\Delta/\Delta}$ cells were observed at 30, 60 and 120 min after plating on FN-coated dishes (Fig. 3A). The mean percentages of flattened cells at each time point are shown in Fig. 3B. The disparity in cell spreading was most apparent 30 min after plating, when more than 70% of the Cas exon $2^{+/+}$ cells had already flattened, while only 37% of Cas exon $2^{\Delta/\Delta}$ cells showed a flattened phenotype. The spreading delay in Cas exon $2^{\Delta/\Delta}$ cells continued and was still observed at 120 min. These results demonstrated that Cas exon $2^{\Delta/\Delta}$ cells had a reduced ability to spread on FN.

The deficiency of Cas exon 2 impaired formation of the FAK/Cas/CrkII complex, tyrosine-phosphorylation of FAK and Cas, and FAK/Src binding on FN

Upon FN stimulation, integrin clustering promotes FAK autophosphorylation at Tyr397, which creates a binding site for the SH2 domain of Src (Mitra *et al.* 2005). FAK/Src binding leads to the conformational activation of Src and results in an activated FAK/Src signaling complex (Schlaepfer *et al.* 2004), which enhances tyrosine-phosphorylation of Cas (Sakai *et al.* 1994; Mitra *et al.* 2005) Tyrosine-phosphorylated Cas binds to CrkII through the SD domain with preference for YDXP motifs (Songyang *et al.* 1993), which subsequently leads to activate downstream small GTP-binding proteins through C3G (Kiyokawa *et al.* 1998a,b; Klemke *et al.* 1998) and plays a key role in cell migration (Fig. 8A).

We then investigated whether the deficiency of Cas exon 2 might affect Cas' association with its major signaling molecules, FAK (Polte & Hanks 1995), Src (Nakamoto *et al.* 1996) and CrkII (Mayer *et al.* 1995) to which Cas binds through its SH3, SBD and SD, respectively. Protein aliquots extracted from Cas exon $2^{+/+}$ and

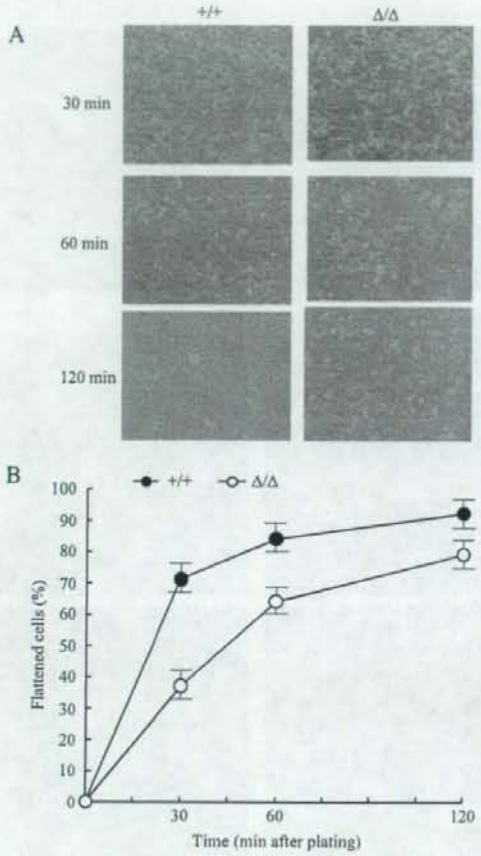

Figure 3 Reduced spreading ability of Cas exon $2^{\Delta/\Delta}$ cells on FN. (A) Photographs of Cas exon $2^{+/+}$ cells and Cas exon $2^{\Delta/\Delta}$ cells at 30, 60 and 120 min after plating on FN-coated dishes. Cells were added to FN-coated dishes and incubated at 37 °C for indicated times. Photographs were taken under a microscope with an objective of 100×. (B) Cell spreading was quantitated by calculating the percentages of spread cells (*error bars* show the standard deviation). Single cells that were phase-bright with rounded morphology were scored non-spread, whereas those that possessed a flattened shape and looked phase-dark were scored as spread. Results presented here are representative mean values of eight independent fields of three experiments.

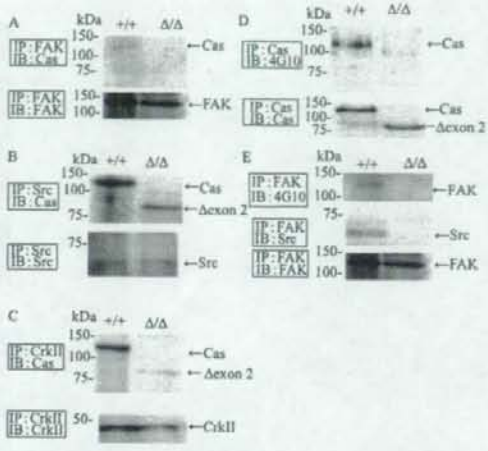

Figure 4 Impaired FAK/Cas/CrkII complex formation, tyrosine-phosphorylation of FAK and Cas, and FAK/Src binding upon FN stimulation in Cas exon $2^{\Delta/\Delta}$ cells. Serum-starved Cas exon $2^{+/+}$ cells and Cas exon $2^{\Delta/\Delta}$ cells were cultured on FN-coated dishes for 1 h, harvested and lysed with 1% Triton lysis buffer. (A) FAK immunoprecipitates (IP : FAK) were probed with anti-Cas (IB : Cas) or anti-FAK (IB : FAK). (B) Src immunoprecipitates (IP : Src) were probed with anti-Cas (IB : Cas) or anti-Src (IB : Src). (C) CrkII immunoprecipitates (IP : CrkII) were probed with anti-Cas (IB : Cas) or anti-CrkII (IB : CrkII). (D) Cas immunoprecipitates (IP : Cas) were probed with 4G10 (IB : 4G10) or anti-Cas (IB : Cas). (E) FAK immunoprecipitates (IP : FAK) were probed with 4G10 (IB : 4G10), anti-Src (IB : Src) or anti-FAK (IB : FAK).

Cas exon $2^{\Delta/\Delta}$ cells plated on FN were immunoprecipitated with antibodies against either FAK, Src or CrkII and immunoprecipitated proteins were blotted with anti-Cas2. As shown in Fig. 4A, wild-type Cas was associated with FAK, whereas Cas Δexon 2 could not bind to FAK. By contrast, Fig. 4B shows that Src bound to both Cas and Cas Δexon 2 at similar levels. We then analyzed possible alteration in CrkII binding to Cas in Cas exon $2^{\Delta/\Delta}$ cells. As shown in Fig. 4C, in Cas exon $2^{+/+}$ cells, stable complex formation of Cas and CrkII was detected, whereas in Cas exon $2^{\Delta/\Delta}$ cells, the binding activity of CrkII to Cas Δexon 2 was significantly reduced. We then analyzed whether the deficiency of Cas exon 2 might affect tyrosine-phosphorylation of Cas. As shown in Fig. 4D, Cas Δexon 2 was not tyrosine-phosphorylated upon FN stimulation. In addition, we could not detect FAK tyrosine-phosphorylation and FAK/Src binding (Fig. 4E). These results indicated that Cas exon 2-deficiency impaired formation of the FAK/Cas/CrkII complex, tyrosine-phosphorylation of FAK and Cas, and FAK/Src binding upon FN stimulation.

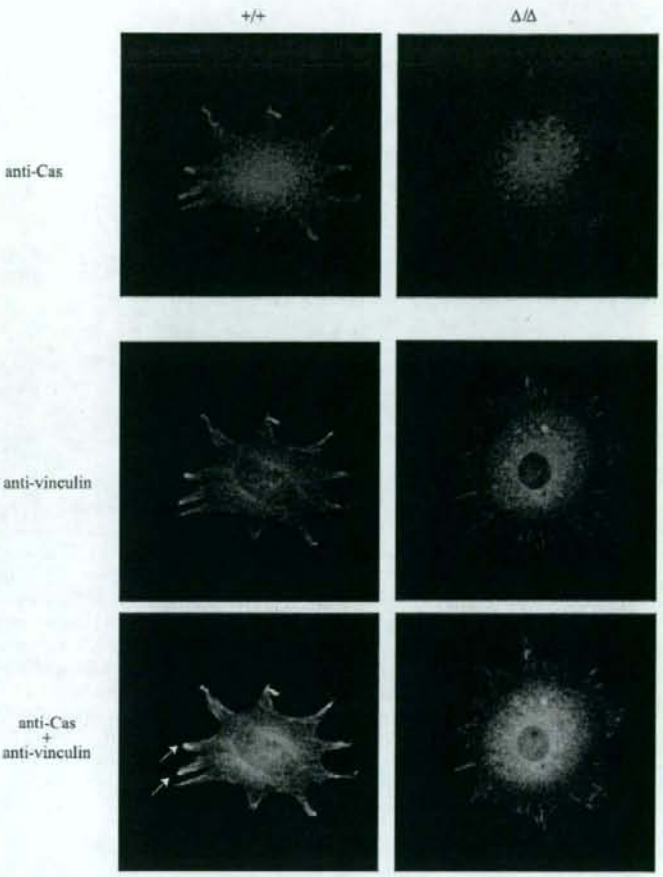

Figure 5 Cas exon 2 is required for the localization of Cas to focal adhesions upon FN stimulation. Cas exon $2^{+/+}$ and Cas exon $2^{\Delta/\Delta}$ cells grown on FN-coated coverslips were stained with anti-Cas and anti-vinculin (hVIN-1) antibodies. Texas red-labeled secondary antibody targeted the anti-Cas antibody and Fluorescein-labeled secondary antibody labeled the anti-vinculin antibody. Following FN stimulation, wild-type Cas was recruited to focal adhesions, as demonstrated by the yellow double staining pattern (left lower panel, indicated by *arrows*), whereas Cas Δexon 2 remained in the cytoplasm and did not concentrate at focal adhesions (right lower panel).

Cas exon 2 is required for the localization of Cas to focal adhesions upon FN stimulation

We compared the subcellular localization of wild-type Cas and Cas Δexon 2 in primary fibroblasts stimulated by FN. Cas exon $2^{+/+}$ and Cas exon $2^{\Delta/\Delta}$ cells grown on FN-coated coverslips were stained with an anti-Cas2. Anti-vinculin (hVIN-1) staining was also performed to identify focal adhesions. As shown in Fig. 5, following FN stimulation, wild-type Cas was recruited to focal adhesions as previously reported (Nakamoto *et al.* 1997), as demonstrated by the yellow double staining pattern (Fig. 5, left lower panel, indicated by *arrows*), whereas Cas Δexon 2 was retained mainly in the cytoplasm and was not concentrated at focal adhesions (Fig. 5, right lower panel). The results indicated that Cas exon 2 is required for the localization of Cas to focal adhesions upon FN stimulation.

The deficiency of Cas exon 2 up-regulated cell adhesion-associated genes including CXC Chemokine Receptor-4 (CXCR4), CC Chemokine Receptor-5 (CCR5) and thrombospondin 4 in primary fibroblasts

To further characterize the role of Cas exon 2 in intracellular signaling, we performed microarray analyses to investigate alterations in gene expression caused by Cas exon 2-deficiency. RNA samples extracted from Cas exon $2^{+/+}$, Cas exon $2^{+/\Delta}$ and Cas exon $2^{\Delta/\Delta}$ fibroblasts

(12.5 dpc, two embryos for each genotype) were subjected to microarray analysis as described in Experimental procedures. Gene expression patterns of Cas exon $2^{\Delta/\Delta}$ fibroblasts were compared with those of Cas exon $2^{+/+}$ and Cas exon $2^{+/\Delta}$ cells. The complete microarray data set is available from the gene expression omnibus (GEO) database (accession no. GSE8357). Expressed sequence tags were excluded and genes that showed more than a 3.0-fold change in expression are presented in Table 1. One interesting aspect of the result is that cell migration- and cell adhesion-associated genes, such as chemokine ligands/receptors and thrombospondin, were listed among the genes up-regulated by Cas exon 2-deficiency. We thus confirmed the up-regulation of these genes in Cas exon $2^{\Delta/\Delta}$ fibroblasts by quantitative real-time RT-PCR analysis. The results showed that the expression levels of three genes, CXCR4, CCR5 and thrombospondin 4, were significantly enhanced by Cas exon 2-deficiency. The changes in expression measured by microarray analysis correlated well with data from quantitative real-time RT-PCR analyses (Fig. 6). These results demonstrated that the loss of Cas exon 2 induced expression of CXCR4, CCR5 and thrombospondin 4, genes involved in cell motility in primary fibroblasts.

Phospho-IκBα level was augmented in Cas exon $2^{\Delta/\Delta}$ fibroblasts

We then examined the underlying molecular mechanism for the up-regulated expression of CXCR4 and CCR5 in Cas exon $2^{\Delta/\Delta}$ fibroblasts. It is already demonstrated that the extracellular signal-activated transcription factor nuclear factor-κB (NF-κB) regulates the expression of some chemokine ligands/receptors, including CXCR4 (Helbig *et al.* 2003; Kukreja *et al.* 2005) and CCR5 (Kim *et al.* 2006). Activation of NF-κB requires phosphorylation of IκBα. Thus, we compared phospho-IκBα levels between Cas exon $2^{+/+}$ and Cas exon $2^{\Delta/\Delta}$ fibroblasts. As shown in Fig. 7, the phosphorylation level of IκBα was significantly augmented in Cas exon $2^{\Delta/\Delta}$ cells as compared to Cas exon $2^{+/+}$ cells. These results indicated that that the NF-κB signaling pathway was activated by Cas exon 2 deficiency, which would play a role in up-regulated expression of CXCR4 and CCR5 in Cas exon $2^{\Delta/\Delta}$ fibroblasts.

Discussion

Cas is an adaptor molecule implicated in various biological processes, such as cell adhesion, cell migration, cell apoptosis, cell transformation and bacterial infection (Defilippi *et al.* 2006). Structurally, Cas is an adaptor

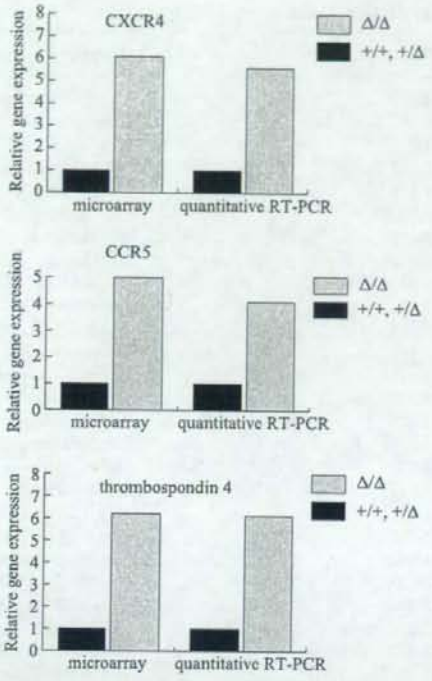

Figure 6 Up-regulated expression of CXCR4, CCR5 and thrombospondin 4 in Cas exon $2^{\Delta/\Delta}$ fibroblasts. RNA samples extracted from Cas exon $2^{+/+}$, Cas exon $2^{+/\Delta}$ and Cas exon $2^{\Delta/\Delta}$ fibroblasts (12.5 dpc, three embryos for each genotype) were used. The changes in expression levels determined by microarray (left) or quantitative real-time RT-PCR (right) are shown.

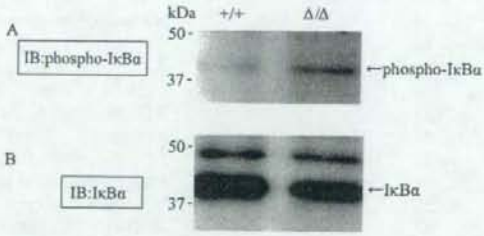

Figure 7 Increased phosphorylation of IκBα in Cas exon $2^{\Delta/\Delta}$ fibroblasts. Cas exon $2^{+/+}$ cells and Cas exon $2^{\Delta/\Delta}$ cells were harvested and lysed with 1% Triton lysis buffer. Equal amounts of total cell lysates were blotted with anti-phospho-IκBα (A) or an anti-IκBα (B).

Table 1 (A) Genes up-regulated in Cas exon $2^{\Delta/\Delta}$ fibroblasts

Fold change	Description	UniGene
46.72	Jumonji, AT rich interactive domain 1D (Rbp2 like)	Mm.262676
12.8	Chemokine (C–C motif) ligand 12	Mm.867
11.2	Killer cell lectin-like receptor, subfamily A, member 2	Mm.4783
7.812	SPARC-like 1 (mast9, hevin)	Mm.29027
6.172	Thrombospondin 4	Mm.20865
6.06	Chemokine (C–C motif) receptor 5	Mm.14302
5.988	Astrotactin 1	Mm.329586
5.714	EGF-like-domain, multiple 6	Mm.37707
5.263	Chemokine (C–C motif) ligand 3	Mm.1282
5.102	Chemokine (C–C motif) ligand 9	Mm.2271
5.025	Chemokine (C–X–C motif) receptor 4	Mm.1401
4.484	Lipoprotein lipase	Mm.1514
4.444	Carbonic anhydrase 2	Mm.1186
4.405	SLAM family member 7	Mm.164642
4.405	RAS-like, estrogen-regulated, growth-inhibitor	Mm.46233
4.149	Macrophage scavenger receptor 1	Mm.239291
4	Odd-skipped related 2 (*Drosophila*)	Mm.46336
3.984	X-linked lymphocyte-regulated 3a	Mm.195091
3.921	C-type lectin domain family 14, member a	Mm.280563
3.831	Schlafen 8	Mm.347694
3.802	Interferon activated gene 203	Mm.261270
3.623	G-protein coupled receptor 65	Mm.378924
3.584	Hepatitis A virus cellular receptor 2	Mm.72168
3.571	Sciellin	Mm.244003
3.333	Adrenomedullin receptor	Mm.2857
3.257	Matrix metalloproteinase 12	Mm.2055
3.236	Cytochrome b-245, β polypeptide	Mm.200362
3.205	Interferon, α-inducible protein 27	Mm.271275
3.195	Prostaglandin E receptor 2 (subtype EP2)	Mm.4630
3.185	Mannose receptor, C type 1	Mm.2019
3.175	Complement component 2 (within H-2S)	Mm.283217
3.155	C-type lectin domain family 4, member d	Mm.299633
3.115	Disabled homolog 2 (*Drosophila*)	Mm.240830

(B) Genes down-regulated in Cas exon $2^{\Delta/\Delta}$ fibroblasts

Fold change	Description	UniGene
−14.19	Xlr-related, meiosis regulated	Mm.14300
−14.17	Kallikrein 24	Mm.378954
−8.397	RIKEN cDNA E130012A19 gene	Mm.24506
−7.892	Vomeronasal 1 receptor, D7	Mm.160377
−7.051	RIKEN cDNA 4933413N12 gene	Mm.158581
−6.949	Probasin	Mm.8034
−6.489	Fibroblast growth factor 16	Mm.154768
−6.432	Phosphatidylinositol glycan, class H	Mm.281044
−5.785	Interleukin-1 receptor-associated kinase 4	Mm.279655
−5.717	RIKEN cDNA 4921517J23 gene	Mm.291129
−5.645	Forkhead box A1	Mm.4578
−5.54	RIKEN cDNA 4931406I20 gene	Mm.318331
−5.344	Phosphatase, orphan 1	Mm.133075
−5.058	RIKEN cDNA 1700020N01 gene	Mm.54306
−5.029	myosin, heavy polypeptide 1, skeletal muscle	Mm.340118

Continued overleaf

Table 1 *Continued*

Fold change	Description	UniGene
−4.676	Thyrotropin releasing hormone receptor	Mm.309350
−4.635	Elongation protein 4 homolog (*S. cereviniae*)	Mm.33870
−4.213	Leukotriene A4 hydrolase	Mm.271071
−4.191	Serine dehydratase-like	Mm.5162
−4.171	Actin related protein M2	Mm.30958
−4.135	Component of Sp100-rs	Mm.362648
−4.058	RIKEN cDNA C230093N12 gene	Mm.4065
−3.843	Procollagen, type II, α1	Mm.2423
−3.734	Calcitonin receptor-like	Mm.75467
−3.528	SRY-box containing gene 10	Mm.276739
−3.46	Profilin 3	Mm.348015
−3.436	Defensin β7	Mm.207067
−3.329	Titin-cap	Mm.10762
−3.329	Melanocortin 3 receptor	Mm.57183
−3.311	Flavin containing monooxygenase 1	Mm.976
−3.271	RIKEN cDNA 2410017P07 gene	Mm.338605
−3.231	Transketolase-like 1	Mm.25057
−3.216	Expressed sequence AU041707	Mm.200898
−3.211	Chromobox homolog 1 (*Drosophila* HP1 β)	Mm.29055
−3.104	Deleted in azoospermia-like	Mm.280641
−3.045	Forkhead box G1	Mm.4704

molecule composed of SH3, SD and SBD (Fig. 1A), and exerts its biological function by interacting various intracellular molecules, such as FAK, CrkII and Src, through its different functional domains. In this paper, to primarily focus on the role of Cas SH3 in cellular function, we established and analyzed primary fibroblasts from mice that were engineered to produce truncated Cas lacking the exon 2-derived region containing the whole SH3 domain (Cas Δexon 2).

As expected from a previous study (Polte & Hanks 1995), we demonstrated that Cas Δexon 2 lost its ability to bind to FAK but retained the ability to bind to Src, irrespective of FN stimulation (Fig. 4A and B and data not shown). In addition, we found that upon FN stimulation, the binding activity of Cas Δexon 2 to CrkII was significantly reduced (Fig. 4C). This result seems curious since the YDXP motifs in the SD, that are the preferred binding site to the CrkII SH2 domain when phosphorylated (Songyang *et al.* 1993), are all conserved in Cas Δexon 2. To investigate the underlying mechanism, we analyzed tyrosine-phosphorylation of Cas between two types of cells. Upon FN stimulation, Cas was apparently tyrosine-phosphorylated in Cas exon $2^{+/+}$ cells as previously reported (Nojima *et al.* 1995), whereas we could not detect tyrosine-phosphorylation of Cas Δexon 2 in Cas exon $2^{\Delta/\Delta}$ cells (Fig. 4D). In addition, we examined tyrosine-phosphorylation of FAK, which is the primary event following integrin stimulation. Surprisingly, FAK was not tyrosine-phosphorylated in Cas exon $2^{\Delta/\Delta}$ cells (Fig. 4E). Furthermore, FAK/Src binding was not detected in Cas exon $2^{\Delta/\Delta}$ cells (Fig. 4E), probably owing to impaired tyrosine-phosphorylation of FAK. These results indicate that Cas exon 2 is essential for FAK auto-phosphorylation upon FN. This idea is in line with a previous study, in which Cas lacking SH3 failed to bind to CrkII, which subsequently abolished FAK/Cas/CrkII complex formation as well as FAK auto-phosphorylation by FN (Iwahara *et al.* 2004). The underlying mechanism for impaired tyrosine-phosphorylation of FAK in Cas exon $2^{\Delta/\Delta}$ cells remains unclear. One possibility is that the constitutive FAK/Cas binding might be essential for conformational change of FAK tyrosine-phosphorylation. Alternatively, the FAK/Cas complex formation might be required for FAK to keep the tyrosine-phosphorylated state. A previous study showed that CrkII knockdown reduces integrin-stimulated FAK Tyr397 autophosphorylation (Iwahara *et al.* 2004). Therefore, the Cas/CrkII complex may also affect tyrosine-phosphorylation of FAK as an upstream regulator in reverse (Iwahara *et al.* 2004).

We also compared the intracellular localization of Cas and Cas Δexon 2 upon FN stimulation. In contrast to Cas to be localized to focal adhesions as previously reported (Nakamoto *et al.* 1997), no clear localization of

Cas Δexon 2 at focal adhesions was found (Fig. 5). Impaired recruitment of Cas to focal adhesions following FN stimulation was reported in Src-deficient cells (Nakamoto *et al.* 1997), and Src can be regarded as a recruiting molecule of Cas to focal adhesions (Kaplan *et al.* 1995; Honda *et al.* 1999). Although Cas Δexon 2 and wild-type Cas have comparable binding abilities to bind Src (Fig. 4B), Cas Δexon 2 was not found in focal adhesions (Fig. 5), indicating that Cas exon 2 plays an essential role in the localization of Cas to focal adhesions upon FN stimulation. This idea is supported by our previous finding that Cas lacking SH3 failed to localize at focal adhesions on FN stimulation when expressed in COS-7 cells (Nakamoto *et al.* 1997). While the mechanism is not clear, one possibility is that when Cas Δexon 2 is recruited to focal adhesions by Src, FAK is not tyrosine-phosphorylated and cannot bind to Cas Δexon 2 and Src, which in turn would allow release of Cas Δexon 2 from focal adhesions. Another possibility is that the impaired FAK/Src complex leads to reduced activation of Src, which could not recruit Cas Δexon 2 to focal adhesions. It is possible that impaired tyrosine-phosphorylation of FAK and Cas leads to incomplete formation of FAK/Cas/Src/CrkII complex and impaired localization of Cas to focal adhesions, which resulted in delayed cell migration (Fig. 2) and spreading on FN (Fig. 3). A previous study using the Cas SD mutants and examining their ability to heal the wound revealed that the effective wound healing was achieved by Cas variants containing at least four of the YDXP/YAVP motifs, the major phosphorylation sites of Cas SD (Shin *et al.* 2004). Since YDXP/YAVP motifs, which serve main binding sites to CrkII, are all conserved in Cas exon $2^{\Delta/\Delta}$ cells (see Fig. 1A), it would be unlikely that the reduced motility is due to the lack of YLVP/YQXP motifs existing in exon 2. In addition, we found that the defects observed in Cas exon $2^{\Delta/\Delta}$ cells were less apparent than those in $Cas^{-/-}$ cells (Honda *et al.* 1999). The reason might be that since Cas exon $2^{\Delta/\Delta}$ cells retain the YDXP/YAVP motifs and the SBD as compared to $Cas^{-/-}$ cells, these domains would partly participate in downstream signaling. In fact, a slight amount of CrkII could bind to Cas upon FN stimulation (Fig. 4C).

To identify downstream molecules regulated by Cas exon 2, we investigated the expression profile of Cas exon $2^{\Delta/\Delta}$ fibroblasts using microarray methods (Table 1). Interestingly, we found that cell migration- and cell adhesion-associated genes, such as chemokine ligands/receptors and thrombospondin, were up-regulated by Cas exon 2 deficiency. We previously compared the expression profile of $Cas^{-/-}$ fibroblasts with that in Cas-re-expressing fibroblasts using the same methods (Nakamoto *et al.* 2002), but could not detect changes in expression of chemokine ligands/receptors and thrombospondins. Thus, the expression changes in these genes (chemokine ligands/receptors and thrombospondins) may be specifically regulated by Cas exon 2-mediated signals.

We also demonstrated that the phospho-IκBα level was augmented in Cas exon $2^{\Delta/\Delta}$ cells, indicating that the NF-κB signaling pathway was activated by Cas exon 2 deficiency (Fig. 7). Based on this result, it is conceivable that up-regulated expression of CXCR4 and CCR5 in Cas exon $2^{\Delta/\Delta}$ fibroblasts is, at least in part, dependent on IκBα phosphorylation. The mechanism underlying the activation of NF-κB signaling and up-regulated expression of CXCR4 and CCR5 is not clear. One possibility is that since the 5′-promoter region of FAK contains NF-κB binding sites, the NF-κB transcription factor might play a role in regulating FAK transcription (Golubovskaya *et al.* 2004). It would also be possible that NF-κB is activated to compensate for the impaired tyrosine-phosphorylation of FAK and FAK/Cas binding in Cas exon $2^{\Delta/\Delta}$ cells.

In summary, we demonstrated that Cas exon 2 plays an essential role in cell migration, cell spreading on FN, tyrosine-phosphorylation of FAK and Cas, FAK/Cas/Src/CrkII complex formation and recruitment of Cas to focal adhesions in primary fibroblasts. In addition, we showed that Cas exon 2-deficiency significantly up-regulated expression of CXCR4 and CCR5, molecules implicated in cell motility (Fig. 8). Our findings define the biological roles of Cas exon 2 and provide novel insights into Cas SH3 function in intracellular signaling.

Experimental procedures

Antibodies

A polyclonal antibody against Cas, anti-Cas2, was generated as previously described (Sakai *et al.* 1994). Antibodies against FAK, Src and CrkII were from Santa Cruz Biotechnology, Santa Cruz, CA, anti-phosphotyrosine antibody 4G10 was from Upstate Biotechnology, Lake Placid, NY and hVIN-1 was from Sigma, St. Louis, MO. Anti-IκBα and anti-phospho-IκBα were from Cell Signaling Technology, Danvers, MA. Anti-Fluorescein-labeled and Texas red-labeled secondary antibodies were from Invitrogen, Carlsbad, CA.

Cultivation of primary fibroblasts

Cas exon $2^{+/\Delta}$ mice were intercrossed and embryos at 12.5 dpc were collected. Heads and internal organs were used for genotyping and primary embryonic fibroblasts were isolated from the remaining of embryos and cultured in Dulbecco's modified Eagle's

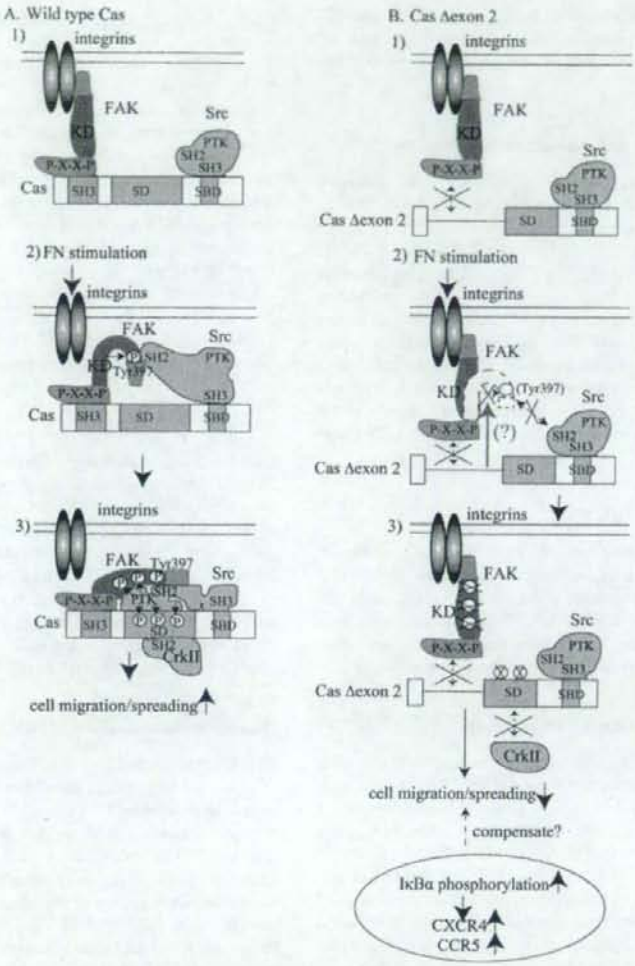

Figure 8 (A) Models for a signaling network involving wild-type Cas. (1) Cas binds to the proline-rich region of FAK through its SH3 domain and binds to the SH3 domain of Src through its Src binding domain (SBD) in unstimulated cells. (2) Upon FN stimulation, integrin clustering promotes FAK autophosphorylation at Tyr397, which creates a binding site for the SH2 domain of Src. (3) FAK/Src binding leads to the conformational activation of Src and results in an activated FAK/Src signaling complex. FAK/Cas binding and activated Src are linked to enhanced tyrosine-phosphorylation of Cas. Tyrosine-phosphorylated Cas binds to CrkII SH2 domain through the SD domain with preference for YDXP motifs and the Cas/CrkII complex plays a key role in cell migration/spreading. (B) Models for a signaling network involving Cas Δexon 2. (1) Cas Δexon 2 binds to Src but cannot bind to FAK in unstimulated cells because Cas binds to proline-rich region of FAK through its SH3 domain, which is missing from Cas Δexon 2. (2) Upon FN stimulation, FAK cannot be auto-phosphorylated by an unknown mechanism (possibly involving Cas SH3) and fails to bind to the SH2 domain of Src. Impaired FAK/Src complex leads to reduced activation of the FAK/Src signaling complex. (3) Because FAK is not tyrosine-phosphorylated and Src is not activated, Cas Δexon 2 cannot be tyrosine-phosphorylated and binding of CrkII to Cas Δexon 2 is impaired. Owing to impaired FAK/Cas/Src/CrkII complex, Cas exon 2-deficiency results in delay in cell migration/spreading. Cas exon 2-deficiency also enhances the expression of CXCR4 and CCR5, which may be dependent on IκBα phosphorylation. These factors may be up-regulated to compensate for the cellular functions affected by Cas exon 2-deficiency.

medium (DMEM) with 10% fetal bovine serum (FBS), penicillin (100 U/mL) and streptomycin (100 μg/mL) at 37 °C with 5% CO_2. Experiments were performed between three and five passages.

Immunoblotting and immunoprecipitation

Immunoblotting and immunoprecipitation were performed essentially as previously described (Huang *et al.* 2002). Proteins were extracted by lysing cells in ice-cold 1% Triton lysis buffer [50 mM Tris–HCl PH 8.0, 150 mM NaCl, 1% Triton X-100, 100 mM NaF, 1 mM Na_3VO_4]. For Western blotting, samples were separated by SDS-PAGE and probed with indicated antibodies. Positive signals were visualized with an enhanced chemiluminescence system (Amersham, Uppsala, Sweden). For immunoprecipitation, 500 μg protein aliquots were incubated with the indicated antibodies for 2 h at 4 °C and subsequently with Protein A-Sepharose (Invitrogen) for 1 h at 4 °C. Beads were washed 4 times with 1% Triton lysis buffer and boiled in sample buffer prior to SDS-PAGE analysis.

Cell stimulation with FN

Serum-starved cells were removed from the culture dishes by 0.05% trypsin treatment and were resuspended in DMEM. Culture dishes were coated overnight with 10 μg/mL FN (Chemicon, Temecula, CA) at 4 °C. The suspended cells were then plated on FN-coated dishes and incubated at 37 °C for various periods of time as described previously (Iwahara *et al.* 2004).

Wound healing cell migration assay

The wound healing cell migration assay was performed according to a method used previously (Honda *et al.* 1999). In brief, cells were first grown to confluence in plastic culture dishes, and a wound was made in the cell monolayer using a sterile micropipette tip. Then cells were washed 3 times with PBS and cultured at 37 °C in DMEM containing 10% FBS. Cell movement was assessed 3, 6, 9 and 12 h after wounding. The percentage of reduced distance between the nuclei of cells at each time period relative to the distance between two rims in the cleared field at the beginning was taken as the index.

Cell spreading assay

The cell spreading assay was performed as previously described (Honda *et al.* 1999). In brief, serum-starved cells were removed from the culture dishes by exposure to 0.05% trypsin–EDTA, and 2×10^5 cells in a volume of 1 mL DMEM were added to 35 mm tissue culture dishes coated with 10 μg/mL FN. The dishes were incubated at 37 °C for the indicated periods of time. Single cells that were phase-bright with rounded morphology were scored as non-spread, whereas those that possessed a flattened shape and looked phase-dark were scored as spread. The number of spread cells was calculated as percentage of the total cells in eight independent fields.

Immunofluorescence

Immunofluorescence was performed as previously described (Nakamoto *et al.* 1997). Cells were grown on FN-coated coverslips (Matsunami, Osaka, Japan) for 90 min. They were washed 3 times with phosphate-buffered saline (PBS) and fixed with 3.7% formaldehyde in PBS. The fixed cells were washed twice with PBS and permealized with 0.2% Triton-X in PBS. The cells were rinsed and then blocked in PBS plus 3% bovine serum albumin (Sigma). Primary antibodies were used at the following dilutions for 3 h at room temperature in a humidified chamber: 1 : 200 for anti-Cas2, and 1 : 200 for hVIN-1. The coverslips were washed 3 times with PBS and treated with secondary antibodies at the recommended dilutions. After three washes with PBS, the coverslips were mounted in a 1 : 2 mixture of glycerol and PBS. The cells were examined with a LSM5 PASCAL confocal microscopic system (Carl Zeiss, Germany).

Microarray analysis

Total RNA was extracted from primary fibroblasts using TRIzol Reagent (Invitrogen) according to the manufacturer's protocol. Two micrograms of total RNA from each sample were labeled using One-cycle Target Labeling and Control Reagents (Affymetrix, Santa Clara, CA) and hybridized with a GeneChip slide (Mouse Genome 430 2.0 Array, Affymetrix). Hybridization was performed at 45 °C for 16 h. After hybridization, slides were washed, dried and scanned using the GeneChip Scanner 3000 (Affymetrix). The array results were analyzed using GeneSpring (Agilent Technologies, Santa Clara, CA).

Quantitative real-time RT-PCR analysis

To confirm the differences in expression levels of the genes identified, we used fluorescent-based quantitative real-time RT-PCR with a TaqMan probe. RT-PCR was performed in 20 μL reaction mixtures containing 4 μL of 5 × LightCycler Taqman Master (Roche), 200 nM each primer and 100 nM Universal Probe-Library probe (Roche, Basel, Switzerland). Amplification reaction was carried out in a 384-well reaction plate in a spectrofluorimetric thermal cycler (ABI PRISM 7900 Sequence Detector, Applied Biosystems, Foster City, CA). A threshold cycle (Ct) for each sample was calculated by the point in which the fluorescence exceeded the threshold limit. To normalize the samples for loading total RNA equivalent, the second real-time PCR assay was performed targeting the 18S ribosomal RNA gene.

Acknowledgements

We thank Ikuko Fukuba for technical assistance regarding microarray and quantitative real-time RT-PCR analyses.

This work was in part supported by Grants-in Aids from the Ministry of Education, Culture, Sports, Science and Technology of Japan, from Tsuchiya Foundation, from the Astellas Foundation for Research on Metabolic Disorders, from the Ichiro Kanehara Foundation, and from Hiroshima University 21st Century Center of Excellence Program for Radiation Casualty Medical Research.

References

Cary, L.A., Han, D.C., Polte, T.R., Hanks, S.K. & Guan, J.L. (1998) Identification of p130Cas as a mediator of focal adhesion kinase-promoted cell migration. *J. Cell Biol.* **140**, 211–221.

Defilippi, P., Di Stefano, P. & Cabodi, S. (2006) p130Cas: a versatile scaffold in signaling networks. *Trends Cell Biol.* **16**, 257–263.

Dolfi, F., Garcia-Guzman, M., Ojaniemi, M., Nakamura, H., Matsuda, M. & Vuori, K. (1998) The adaptor protein Crk connects multiple cellular stimuli to the JNK signaling pathway. *Proc. Natl. Acad. Sci. USA* **95**, 15394–15399.

Garton, A.J., Burnham, M.R., Bouton, A.H. & Tonks, N.K. (1997) Association of PTP-PEST with the SH3 domain of p130cas; a novel mechanism of protein tyrosine phosphatase substrate recognition. *Oncogene* **15**, 877–885.

Golubovskaya, V., Kaur, A. & Cance, W. (2004) Cloning and characterization of the promoter region of human focal adhesion kinase gene: nuclear factor κB and p53 binding sites. *Biochim. Biophys. Acta* **1678**, 111–125.

Helbig, G., Christopherson, K.W., 2nd, Bhat-Nakshatri, P., Kumar, S., Kishimoto, H., Miller, K.D., Broxmeyer, H.E. & Nakshatri, H. (2003) NF-κB promotes breast cancer cell migration and metastasis by inducing the expression of the chemokine receptor CXCR4. *J. Biol. Chem.* **278**, 21631–21638.

Honda, H., Nakamoto, T., Sakai, R. & Hirai, H. (1999) p130Cas, an assembling molecule of actin filaments, promotes cell movement, cell migration, and cell spreading in fibroblasts. *Biochem. Biophys. Res. Commun.* **262**, 25–30.

Honda, H., Oda, H., Nakamoto, T., Honda, Z., Sakai, R., Suzuki, T., Saito, T., Nakamura, K., Nakao, K., Ishikawa, T., Katsuki, M., Yazaki, Y. & Hirai, H. (1998) Cardiovascular anomaly, impaired actin bundling and resistance to Src-induced transformation in mice lacking p130Cas. *Nat. Genet.* **19**, 361–365.

Huang, J., Hamasaki, H., Nakamoto, T., Honda, H., Hirai, H., Saito, M., Takato, T. & Sakai, R. (2002) Differential regulation of cell migration, actin stress fiber organization, and cell transformation by functional domains of Crk-associated substrate. *J. Biol. Chem.* **277**, 27265–27272.

Iwahara, T., Akagi, T., Fujitsuka, Y. & Hanafusa, H. (2004) CrkII regulates focal adhesion kinase activation by making a complex with Crk-associated substrate, p130Cas. *Proc. Natl. Acad. Sci. USA* **101**, 17693–17698.

Kaplan, K.B., Swedlow, J.R., Morgan, D.O. & Varmus, H.E. (1995) c-Src enhances the spreading of $src^{-/-}$ fibroblasts on fibronectin by a kinase-independent mechanism. *Genes Dev.* **9**, 1505–1517.

Kim, H.K., Park, H.R., Sul, K.H., Chung, H.Y. & Chung, J. (2006) Induction of RANTES and CCR5 through NF-κB activation via MAPK pathway in aged rat gingival tissues. *Biotechnol. Lett.* **28**, 17–23.

Kirsch, K.H., Georgescu, M.M. & Hanafusa, H. (1998) Direct binding of p130Cas to the guanine nucleotide exchange factor C3G. *J. Biol. Chem.* **273**, 25673–25679.

Kiyokawa, E., Hashimoto, Y., Kobayashi, S., Sugimura, H., Kurata, T. & Matsuda, M. (1998a) Activation of Rac1 by a Crk SH3-binding protein, DOCK180. *Genes Dev.* **12**, 3331–3336.

Kiyokawa, E., Hashimoto, Y., Kurata, T., Sugimura, H. & Matsuda, M. (1998b) Evidence that DOCK180 up-regulates signals from the CrkII-p130Cas complex. *J. Biol. Chem.* **273**, 24479–24484.

Klemke, R.L., Leng, J., Molander, R., Brooks, P.C., Vuori, K. & Cheresh, D.A. (1998) CAS/Crk coupling serves as a "molecular switch" for induction of cell migration. *J. Cell Biol.* **140**, 961–972.

Kukreja, P., Abdel-Mageed, A.B., Mondal, D., Liu, K. & Agrawal, K.C. (2005) Up-regulation of CXCR4 expression in PC-3 cells by stromal-derived factor-1α (CXCL12) increases endothelial adhesion and transendothelial migration: role of MEK/ERK signaling pathway-dependent NF-κB activation. *Cancer Res.* **65**, 9891–9898.

Liu, F., Hill, D.E. & Chernoff, J. (1996) Direct binding of the proline-rich region of protein tyrosine phosphatase 1B to the Src homology 3 domain of p130Cas. *J. Biol. Chem.* **271**, 31290–31295.

Mayer, B.J., Hirai, H. & Sakai, R. (1995) Evidence that SH2 domains promote processive phosphorylation by protein-tyrosine kinases. *Curr. Biol.* **5**, 296–305.

Mitra, S.K., Hanson, D.A. & Schlaepfer, D.D. (2005) Focal adhesion kinase: in command and control of cell motility. *Nat. Rev. Mol. Cell. Biol.* **6**, 56–68.

Nakamoto, T., Sakai, R., Honda, H., Ogawa, S., Ueno, H., Suzuki, T., Aizawa, S., Yazaki, Y. & Hirai, H. (1997) Requirements for localization of p130cas to focal adhesions. *Mol. Cell. Biol.* **17**, 3884–3897.

Nakamoto, T., Sakai, R., Ozawa, K., Yazaki, Y. & Hirai, H. (1996) Direct binding of C-terminal region of p130Cas to SH2 and SH3 domains of Src kinase. *J. Biol. Chem.* **271**, 8959–8965.

Nakamoto, T., Suzuki, T., Huang, J., Matsumura, T., Seo, S., Honda, H., Sakai, R. & Hirai, H. (2002) Analysis of gene expression profile in p130Cas-deficient fibroblasts. *Biochem. Biophys. Res. Commun.* **294**, 635–641.

Nakamoto, T., Yamagata, T., Sakai, R., Ogawa, S., Honda, H., Ueno, H., Hirano, N., Yazaki, Y. & Hirai, H. (2000) CIZ, a zinc finger protein that interacts with p130cas and activates the expression of matrix metalloproteinases. *Mol. Cell. Biol.* **20**, 1649–1658.

Nojima, Y., Morino, N., Mimura, T., *et al.* (1995) Integrin-mediated cell adhesion promotes tyrosine phosphorylation of p130Cas, a Src homology 3-containing molecule having multiple Src homology 2-binding motifs. *J. Biol. Chem.* **270**, 15398–15402.

Polte, T.R. & Hanks, S.K. (1995) Interaction between focal adhesion kinase and Crk-associated tyrosine kinase substrate p130Cas. *Proc. Natl. Acad. Sci. USA* **92**, 10678–10682.

Prasad, N., Topping, R.S. & Decker, S.J. (2001) SH2-containing inositol 5′-phosphatase SHIP2 associates with the p130Cas adapter protein and regulates cellular adhesion and spreading. *Mol. Cell. Biol.* **21**, 1416–1428.

Sakai, R., Iwamatsu, A., Hirano, N., Ogawa, S., Tanaka, T., Mano, H., Yazaki, Y. & Hirai, H. (1994) A novel signaling molecule, p130, forms stable complexes *in vivo* with v-Crk and

v-Src in a tyrosine phosphorylation-dependent manner. *EMBO J.* **13**, 3748–3756.

Schlaepfer, D.D., Broome, M.A. & Hunter, T. (1997) Fibronectin-stimulated signaling from a focal adhesion kinase-c-Src complex: involvement of the Grb2, p130cas, and Nck adaptor proteins. *Mol. Cell. Biol.* **17**, 1702–1713.

Schlaepfer, D.D., Mitra, S.K. & Ilic, D. (2004) Control of motile and invasive cell phenotypes by focal adhesion kinase. *Biochim. Biophys. Acta* **1692**, 77–102.

Shin, N.Y., Dise, R.S., Schneider-Mergener, J., Ritchie, M.D., Kilkenny, D.M. & Hanks, S.K. (2004) Subsets of the major tyrosine phosphorylation sites in Crk-associated substrate (CAS) are sufficient to promote cell migration. *J. Biol. Chem.* **279**, 38331–38337.

Songyang, Z., Shoelson, S.E., Chaudhuri, M., *et al.* (1993) SH2 domains recognize specific phosphopeptide sequences. *Cell* **72**, 767–778.

Vuori, K., Hirai, H., Aizawa, S. & Ruoslahti, E. (1996) Introduction of p130cas signaling complex formation upon integrin-mediated cell adhesion: a role for Src family kinases. *Mol. Cell. Biol.* **16**, 2606–2613.

Vuori, K. & Ruoslahti, E. (1995) Tyrosine phosphorylation of p130Cas and cortactin accompanies integrin-mediated cell adhesion to extracellular matrix. *J. Biol. Chem.* **270**, 22259–22262.

Received: 24 August 2007
Accepted: 6 November 2007

Hyperphosphorylated Cortactin in Cancer Cells Plays an Inhibitory Role in Cell Motility

Lin Jia, Takamasa Uekita, and Ryuichi Sakai

Growth Factor Division, National Cancer Center Research Institute, Tokyo, Japan

Abstract

Cortactin is frequently overexpressed in cancer cells, and changes of the levels of its tyrosine phosphorylation have been observed in several cancer cells. However, how the expression level and phosphorylation state of cortactin would influence the ultimate cellular function of cancer cells is unknown. In this study, we analyzed the role of cortactin in gastric and breast cancer cell lines using RNA interference technique and found that knockdown of cortactin inhibited cell migration in a subset of gastric cancer cells with a lower level of its tyrosine phosphorylation, whereas it greatly enhanced cell migration and increased tyrosine phosphorylation of p130Cas in other subsets of cells with hyperphosphorylated cortactin. Consistent results were obtained when hyperphosphorylation of cortactin was induced in MCF7 breast cancer cells by expressing Fyn tyrosine kinase. Additionally, immunostaining analysis showed that knockdown of hyperphosphorylated cortactin resulted in the recruitment of p130Cas to focal adhesions. These results suggest that cortactin hyperphosphorylation suppresses cell migration possibly through the inhibition of membrane localization and tyrosine phosphorylation of p130Cas.
(Mol Cancer Res 2008;6(4):654–62)

Introduction

Protein phosphorylation by tyrosine kinases functions as a major switch in cellular biological signaling events through modulating protein-protein interaction and protein conformation. Substrates of Src family kinases (SFK) play essential roles in various cellular events by mediating tyrosine phosphorylation–dependent signals. Because cortactin was originally identified as a v-Src substrate, it has been shown to play a critical role in the organization of the cytoskeleton (1). The cortactin gene *EMS1* is located on chromosome 11q13, a region amplified in several cancers such as head and neck squamous carcinoma and breast cancer (2-6). Cortactin is a modular protein that contains several motifs and domains involved in protein-protein interactions. An NH_2-terminal acidic domain mediates its binding to Arp2/3, which regulates actin assembly, followed by an adjacency of six-and-a-half tandem repeats of 37 amino acids called cortactin repeats domain. There is a proline-rich domain immediately upstream of the SH3 domain, which also contains tyrosine residues phosphorylated by Src family kinases (7, 8). At the carboxyl terminus, there is a Src homology 3 (SH3) domain binding to several proteins, including cortactin binding protein1 (CortBP1/Shank2; ref. 9) and N-WASP (10). Cortactin is a substrate of tyrosine kinases, including SFKs, Fer, and Syk (11-13), and of serine/threonine kinases, including Erk and PAK (14, 15). Among the Src family, Fyn kinase seems to play a specific role in the cortactin function in some tumors because highly phosphorylated cortactin was shown to associate with Fyn kinase in metastatic murine melanoma in our previous study (16). However, how cortactin phosphorylation affects intercellular signaling pathways for cell dynamics control and other functions is not understood.

It has been shown that cell motility involves coordination of multiple signaling pathways regulating cell-substrate adhesion or actin polymerization (17, 18). A docking protein, p130Cas (Crk-associated substrate), is one of the key components of integrin-mediated signaling pathways, which conducts cell migration and actin filament reorganization in a tyrosine phosphorylation–dependent manner (19, 20). The COOH-terminal domain of p130Cas has both consensus SH3 and SH2 domains, binding sites for SFKs, which are mainly responsible for the phosphorylation of p130Cas (21).

In this study, we investigated the role of cortactin in human gastric cancer cell lines using RNA interference technique and discovered that knockdown of cortactin led to suppression of cell migration of the cells in which phosphorylation of cortactin is at basal level, whereas it increased cell migration of the cells in which cortactin is highly phosphorylated. It was also observed that knockdown of cortactin resulted in enhancement of cell motility of breast cancer cell line MCF7 in which phosphorylation level of cortactin was elevated by exogenously introduced Fyn kinase. In both cases, marked elevation in tyrosine phosphorylation of p130Cas was specifically and consistently observed by knockdown of hyperphosphorylated cortactin. We propose that tyrosine phosphorylation of cortactin may function as a molecular switch buffering the change in cell motility.

Results

Effect on Cortactin Knockdown on Cell Migration of Gastric Cancer Cells

Levels of tyrosine phosphorylation of cortactin were examined in human gastric cancer cell lines HSC57,

Received 5/18/07; revised 12/6/07; accepted 12/14/07.
Grant support: Program for Promotion of Cancer Research (Japan) for the Third Term Comprehensive 10-Year-Strategy for Cancer Control.
The costs of publication of this article were defrayed in part by the payment of page charges. This article must therefore be hereby marked *advertisement* in accordance with 18 U.S.C. Section 1734 solely to indicate this fact.
Note: Supplementary data for this article are available at Molecular Cancer Research Online (http://mcr.aacrjournals.org/).
Requests for reprints: Ryuichi Sakai, Growth Factor Division, National Cancer Center Research Institute, 5-1-1 Tsukiji, Chuo-ku, Tokyo 104-0045, Japan. Phone: 81-3-3542-5247; Fax: 81-3-3542-8170. E-mail: rsakai@gan2.res.ncc.go.jp

doi:10.1158/1541-7786.MCR-07-0220

HSC44As3, HSC44PE, and HSC58As9 established in National Cancer Center Research Institute, Japan (22), along with a breast carcinoma cell line MCF7 that possesses amplification of cortactin gene, *EMS1* (2). Expression of total cortactin was at similar levels (Fig. 1A, *bottom*), whereas there was a significant difference in tyrosine phosphorylation among these cell lines (Fig. 1A, *top*). HSC57, HSC44As3, and MCF7 cells exhibited a low level of tyrosine phosphorylation of cortactin, whereas HSC44PE and HSC58As9 showed hyperphosphorylation of cortactin as also indicated by the ratio of tyrosine-phosphorylated cortactin to total cortactin (Fig. 1A).

We knocked down cortactin expression by small interfering RNA (siRNA) to investigate the function of cortactin in the regulation of cell motility in various cancer cells using the Transwell assay. It was confirmed by immunoblotting that >80% of cortactin expression was down-regulated at 72 hours after initiation of siRNA treatment (Fig. 1B). Interestingly, knockdown of cortactin increased cell migration in HSC44PE and HSC58As9 cells with hyperphosphorylated cortactin, whereas it impaired cell motility in HSC57, Hsc44As3, and MCF7 cells with a low level of phosphorylated cortactin (Fig. 1C). Essentially similar effect on cell migration was seen by another siRNA, cort-siRNA2 (data not shown). To further confirm the migration-promoting effect of cortactin siRNA in HSC44PE cells, we expressed mouse cortactin (mcort-WT), which is well conserved to human cortactin by the retrovirus vector (4), along with the mutant mouse cortactin (mcort-Mut), which lacks all three putative tyrosine phosphorylation sites by exchanging tyrosine residues 421, 466, and 482 to phenylalanine (F421F466F482). Wild-type cortactin but not the mutant

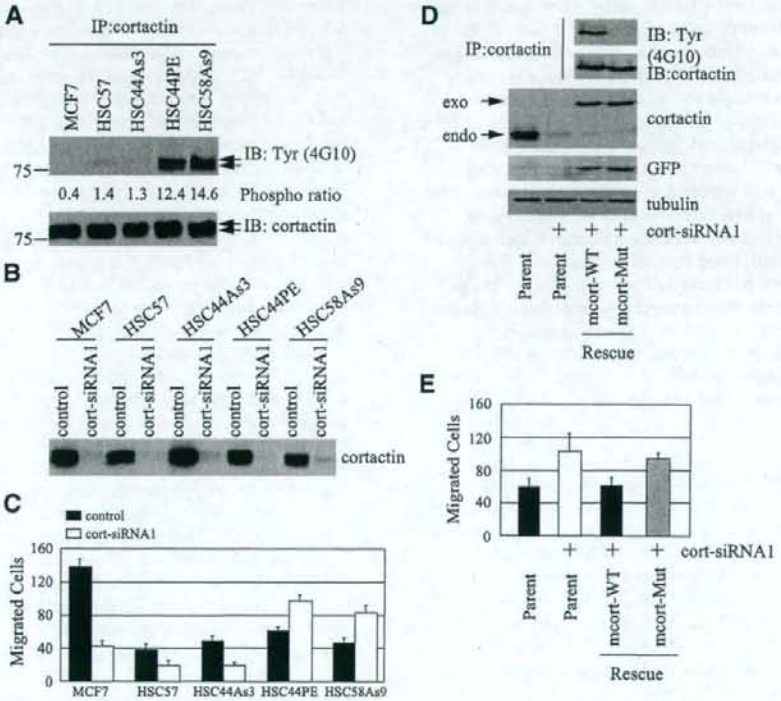

FIGURE 1. Changes in cell motility by knockdown of cortactin in gastric and breast cancer cells. **A.** To evaluate expression and tyrosine phosphorylation of cortactin, cell lysates of gastric and breast cancer cell lines were immunoprecipitated (*IP*) with anti-cortactin antibody (2 μg/mL) and immunoblotted by anti-phosphotyrosine antibody (4G10) and anti-cortactin antibody. Arrows, positions of cortactin isoforms (p85/80). MCF7, HSC57, and HSC44As3 cells exhibited a low level of tyrosine phosphorylation of cortactin, whereas HSC44PE and HSC58As9 showed hyperphosphorylation of cortactin. Quantification of tyrosine-phosphorylated cortactin is noted under the panel. Bottom, the expression of total cortactin. **B.** Amounts of cortactin in these cell lines at 72 h after siRNA treatment. **C.** Cell motility in various cancer cell lines was evaluated by numbers of migrated cells on the membrane. Knockdown of cortactin by siRNA led to inhibition of cell migration in HSC57, HSC44As3, and MCF7 cells with hypophosphorylated cortactin, whereas it resulted in increase of cell migration in HSC44PE and HSC58As9 cells with hyperphosphorylated cortactin. **D.** HSC44PE cells (*Parent*) and HSC44PE cells stably expressed mouse cortactin (*mcort-WT*) or F421F466F482 triple mutant of mouse cortactin (*mcort-Mut*) fused with GFP were treated with or without cortactin siRNA. Cells were lysed 72 h after treatment and immunoblotted for cortactin and GFP. The concentration of total proteins was confirmed by the same membrane rehybridized with anti–α-tubulin antibody. Cortactin siRNA down-regulates endogenous human cortactin (*endo*) but not exogenous mouse cortactins (*exo*). Tyrosine phosphorylation of mouse cortactins was analyzed by immunoprecipitation of total cortactin and immunoblotting with anti-phosphotyrosine antibody (4G10). The quantification of immunoprecipitated cortactin is shown in the bottom (*IB: cortactin*). **E.** Effect of the rescue of mouse cortactin expression on cell migration in cortactin knockdown HSC44PE cells were analyzed as described. Rescue of tyrosine-phosphorylated cortactin (*mcort-WT*) affected the inhibition of cell migration but nontyrosine-phosphorylated cortactin (*mcort-Mut*) did not.

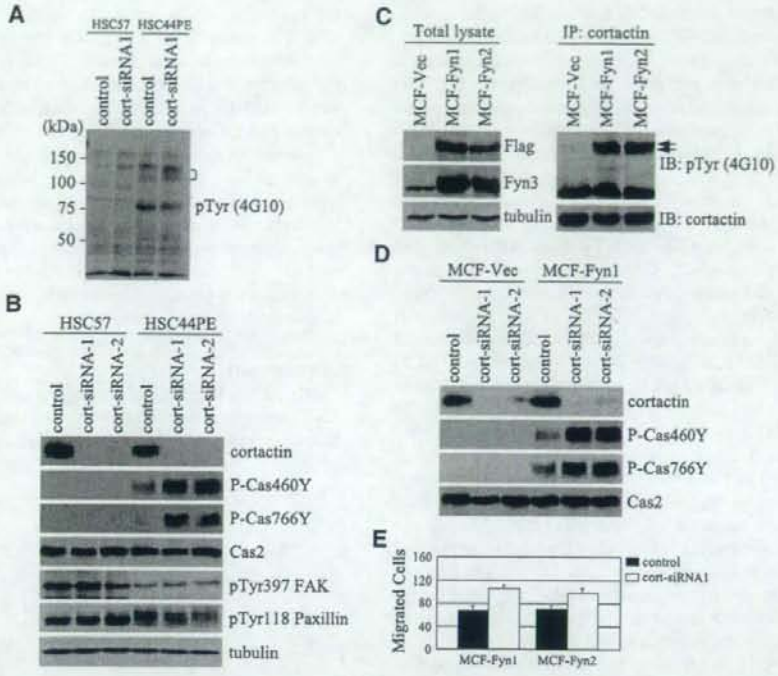

FIGURE 2. Analysis of cell motility in MCF clones with hyperphosphorylated cortactin. **A.** HSC57 and HSC44PE cells were treated with cortactin siRNA for 72 h; the whole-cell lysates were subjected to immunoblotting assay by antibody 4G10 to see phosphotyrosine-containing proteins. The phosphotyrosine-containing protein around 120 to 130 kDa was significantly enhanced (*square bracket*). **B.** Marked elevation of phosphorylation of p130Cas at tyrosine 460 and tyrosine 766 in HSC44PE cells was confirmed by specific anti–phospho-Cas antibodies (P-Cas460Y and P-Cas766Y) using two independent cortactin siRNAs. Immunoblotting by anticortactin, anti-Cas2, anti–phospho-FAK (Tyr^{397}), anti–phospho-paxillin (Tyr^{118}), and anti-tubulin antibodies are also shown. **C.** Stable clones of MCF7 cells expressing Flag-tagged Fyn kinase (MCF-Fyn1 and MCF-Fyn2) or vector alone (MCF-Vec) were established (see Materials and Methods). Left, immunoblotting by anti-Flag, anti-Fyn3, and anti-tubulin antibodies to show high expression of Flag-Fyn in these clones. Right, the tyrosine phosphorylation of cortactin was markedly induced in MCF-Fyn1 and MCF-Fyn2 clones with no significant change in total cortactin expression. **D.** The enhancement of phosphorylation of p130Cas at tyrosine 460 and tyrosine 766 in MCF-Fyn1 cells treated with two independent cortactin siRNAs was confirmed by specific anti–phospho-Cas antibodies (P-Cas460Y and P-Cas766Y). **E.** The effect of cortactin siRNA on cell migration of MCF7-Fyn clones was analyzed as described.

cortactin could block the elevation of cell migration induced by siRNA of cortactin in HSC44PE cells, suggesting that cortactin is actually suppressing migration of HSC44PE cells in a tyrosine phosphorylation–dependent manner. These results indicate that cortactin might differentially exert negatively and positively regulating functions in cell migration depending on its tyrosine phosphorylation.

Cortactin was originally identified as a substrate of SFKs. Among SFKs expressing in solid tumor cells, Fyn kinase was shown to play central roles in the tyrosine phosphorylation of cortactin in murine melanoma cells in our previous study (16). Treatment by a Src family specific inhibitor PP2 significantly reduced tyrosine phosphorylation of cortactin in HSC44PE cells (Supplementary Fig. S1A), suggesting that Src family kinases are actually responsible for tyrosine phosphorylation of cortactin in HSC44PE cells. Relatively high expression of Fyn kinase along with stable association between Fyn and cortactin was observed in HSC44PE cells (Supplementary Fig. S1B and S1C), suggesting the possibility that Fyn kinase is involved in hyperphosphorylation of cortactin in HSC44PE cells.

Knockdown of Cortactin Enhanced Tyrosine Phosphorylation of p130Cas in the Cells with Hyperphosphorylation of Cortactin

By knockdown of cortactin, tyrosine phosphorylation of a 125 to 130 kDa protein was remarkably enhanced in HSC44PE cells but not in HSC57 cells (Fig. 2A). In HSC44PE cells treated with cortactin siRNA, dramatically increased tyrosine phosphorylation of p130Cas was observed using phosphospecific antibody of p130Cas (P-Cas460Y) at the exactly same position where the 125 to 130 kDa protein was detected by 4G10 (Fig. 2B), whereas anti–phospho-FAK (Tyr^{397}) and phospho-paxillin (Tyr^{118}) antibodies failed to detect a significant change of phosphorylation state (Fig. 2B). We also generated another phosphospecific antibody against p130Cas (P-Cas766Y; see Materials and Methods), and found consistent elevation in tyrosine phosphorylation of p130Cas by P-Cas766Y antibody in HSC44PE cells treated with two independent siRNAs for cortactin (Fig. 2B). On the other hand, the level of phosphorylation of p130Cas was not significantly elevated in HSC57 cells (Fig. 2B). There were no clear changes

in the phosphorylation level of FAK or paxillin by the cortactin siRNAs in either HSC44PE cells or HSC57 cells (Fig. 2B).

To confirm the role of hyperphosphorylated cortactin in these cells, we also generated MCF7 cell lines that have elevated tyrosine phosphorylation of cortactin. Original MCF7 cells showed high expression of cortactin with the minimum level of tyrosine phosphorylation (Fig. 1A) and low expression of Fyn kinase (Fig. 2C). A vector expressing the Flag-tagged Fyn kinase was introduced into MCF7 cells, and several clones with stable expression of Fyn kinase were isolated, and two of these clones were named as MCF-Fyn1 and MCF-Fyn2. The amount of Fyn protein in both cells was ~10-fold greater than that of endogenous Fyn kinase in original MCF7 cells (Fig. 2C). Marked hyperphosphorylation of cortactin was observed in these two clones where Fyn kinase was introduced whereas original MCF7 cells or mock-transfected cells (MCF-Vec) were not (Fig. 2C). Knockout of cortactin greatly enhanced tyrosine phosphorylation of p130Cas both in MCF-Fyn1 cells and MCF-Fyn2 cells but not in MCF7-Vec cells (Fig. 2D and data not shown). These consistent results suggest that hyperphosphorylated cortactin may inhibit tyrosine phosphorylation of p130Cas in both HSC44PE and MCF-Fyn cells. Knockdown of cortactin also increased cell motility in both MCF-Fyn1 and MCF-Fyn2 cells whereas it blocked cell migration in parental MCF7 cells and MCF-Vec cells (Figs. 1C and 2E; data not shown). Similar results were obtained in the study using gastric cancer cells and it was shown that hyperphosphorylation of cortactin switches the response of cell motility.

Because many reports have shown the significant role of phosphorylation of p130Cas in cell migration, we examined whether knockdown of p130Cas by siRNA impairs the cell motility of HSC44PE cells treated or not treated with cortactin siRNA. Double treatment of Cas-siRNA and cort-siRNA completely impaired cell motility as well as treatment by Cas-siRNA alone, showing that p130Cas plays a dominant role in the regulation of cell motility of HSC44PE cells (Fig. 3B). These results indicate the possibility that hyperphosphorylated cortactin may suppress cell migration through inhibiting tyrosine phosphorylation of p130Cas.

Recruitment of p130Cas to Focal Adhesion by Treatment of Cortactin siRNA

To further investigate the cause of tyrosine phosphorylation of p130Cas induced by knockdown of cortactin, we analyzed the subcellular localization of p130Cas, cortactin, and focal adhesion proteins in HSC44PE cells. Total cortactin was widely expressed near the cell membrane in HSC44PE cells (Fig. 4A and B) whereas phosphorylated cortactin detected by a phosphospecific antibody against cortactin Y421 appeared at a specific domain, which seems to be focal adhesion within the cell membrane (Fig. 4B). It was further shown that phosphotyrosine-containing cortactin was clearly colocalized with vinculin, which is expressed at focal adhesion (Fig. 4C). By the treatment with cortactin siRNA, both the signals detected by total cortactin and cortactin Y421 were significantly weakened, suggesting these signals are cortactin specific (Fig. 4A).

In the control cells, p130Cas is mainly distributed in the cytoplasm and only slightly expressed at focal adhesion (Fig. 5B, *top*). When cortactin is knocked down, a substantial amount of p130Cas comes to locate at focal adhesion (Fig. 5B, *bottom*), suggesting the loss of cortactin-induced membrane localization of p130Cas. On the other hand, tyrosine-phosphorylated p130Cas detected by phosphospecific antibody was specifically localized at the focal adhesion although the amount of tyrosine phosphorylation was greatly increased by the suppression of cortactin expression (Fig. 5A). This observation may support the model that tyrosine-phosphorylated cortactin expressed predominantly in focal adhesions interferes with the localization of p130Cas at the focal adhesion, which causes tyrosine-phosphorylated p130Cas. Loss of hyperphosphorylated cortactin could therefore recruit p130Cas to the focal adhesion, which results in tyrosine phosphorylation of p130Cas, followed by enhancement of cell motility.

Discussion

We explored the role of cortactin in cell motility by using RNA interference technique in several gastric cancer cell lines that show various phosphorylation states of cortactin. It was

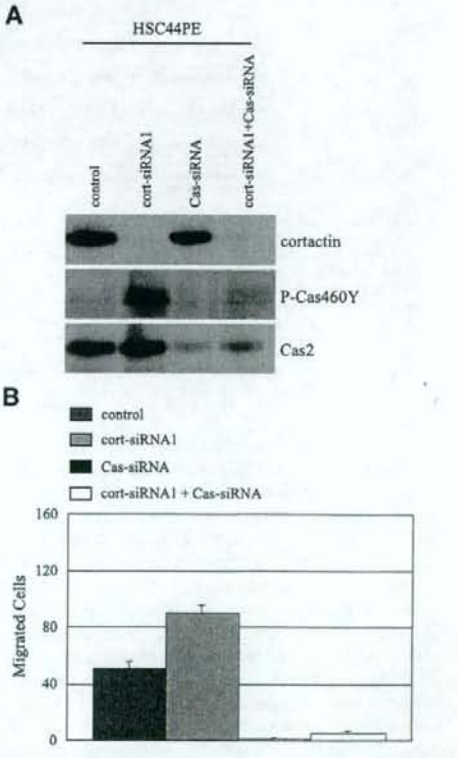

FIGURE 3. Knockdown of p130Cas blocks cell migration of HSC44PE cells regardless of the expression of cortactin. **A** and **B.** HSC44PE cells were treated with either cortactin siRNA or p130Cas siRNA alone, or both, and cell migration was analyzed as described. **A.** Expression of cortactin, p130Cas (Cas2), and phosphorylated p130Cas (pCas460Y) was analyzed to check the effect of each siRNA. **B.** By treatment with siRNA of Cas, cell migration of HSC44PE cells was totally inhibited regardless of the amount of cortactin expression.

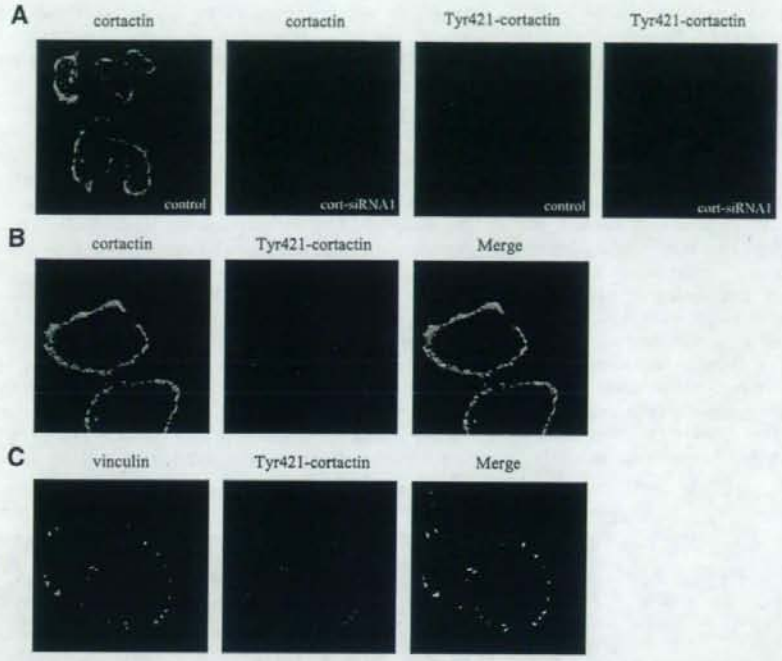

FIGURE 4. Localization of cortactin and tyrosine-phosphorylated cortactin in HSC44PE cells. **A.** HSC44PE cells were transfected with cortactin siRNA or control siRNA for 72 h followed by immunocytostaining with anti-cortactin (*green*) and anti-phospho-cortactin (Tyr^{421}; *red*) antibody. **B.** HSC44PE cells were immunostained with anti-phospho-cortactin (Tyr^{421}; *red*) and anti-cortactin (*green*) antibodies. **C.** HSC44PE cells were immunostained with anti-phospho-cortactin (Tyr^{421}; *red*) and anti-vinculin (*green*) antibodies. Merged image (*Merge*) indicates that tyrosine-phosphorylated cortactin localizes at focal adhesions that are stained by anti-vinculin.

revealed that knockdown of cortactin results in enhanced cell motility along with increased tyrosine phosphorylation of p130Cas in the cells that have hyperphosphorylated cortactin, whereas it impairs cell migration in the cells with a low level of tyrosine-phosphorylated cortactin. In addition, knockdown of hyperphosphorylated cortactin caused recruitment of p130Cas to focal adhesion, which might result in enhanced cell migration. In this study, for the first time, we showed that cortactin has a dual function in the regulation of cell motility, which depends on its tyrosine phosphorylation state.

Amplification and overexpression of the cortactin gene, *EMS1*, have been identified in various cancers (2, 3, 6, 23). In our previous study, overexpression and elevated tyrosine phosphorylation of cortactin was selectively observed in the metastatic subgroup of murine melanoma cells with high migratory potential (16). Based on these results, we first hypothesized that the hyperphosphorylated cortactin may promote cell migration in cancer cells. In this study, gastric cancer cells that have hyperphosphorylated cortactin showed at least similar or higher migration potential compared with those cells with basal levels of tyrosine phosphorylation of cortactin (Fig. 1A and C). However, unexpectedly, knockdown of cortactin in these cells further enhanced cell migration. The effect of cortactin knockdown was opposite in the cells with a low level of cortactin phosphorylation. This paradoxical outcome by cortactin knockdown was also confirmed in breast cancer cells MCF7, which expressed a significant amount of cortactin although the level of tyrosine phosphorylation was quite low. Introduction of Fyn kinase to MCF7 cells significantly enhanced the tyrosine phosphorylation of cortactin. In this condition, loss of cortactin by siRNA enhanced cell migration whereas it had a negative effect on cell migration in the parental cells. Based on this finding, cortactin hyperphosphorylation may be induced as a negative feedback mechanism when cells acquire highly migratory potential.

Some of the studies have shown that knockdown of cortactin results in impaired cell motility in hepatocellular carcinoma and head and neck squamous cell carcinoma cells (24, 25), whereas other studies have shown no significant effect on cell motility (8, 26), although all these studies lack information on the phosphorylation states of cortactin. Because it is suggested that cortactin differentially functions in cell migration depending on its phosphorylation state, the previous controversial results from the knockdown of cortactin should be reevaluated from the viewpoint of its tyrosine phosphorylation state. A previous study shows positive effect of the cortactin phosphorylation on the cell migration by overexpression of normal cortactin and phosphorylation-defective mutants in the endothelial cells (27). Although this study does not mention about the level of tyrosine phosphorylation of endogenous cortactin either, it might be weak in normal endothelial cells. Therefore, the positive effect of cortactin expression shown in the study might be consistent with our result using HSC57 or MCF7 cells, whereas the dominant-negative effect of phosphorylation-defective mutant might indicate some different function of cortactin in the endothelial cells.

In our observation, knockdown of cortactin induced outstanding enhancement in tyrosine phosphorylation of

p130Cas. Because there is no significant change in the phosphorylation of other substrates of SFKs such as FAK and paxillin, it is indicated that there exists some specific mechanism underlying the regulation of tyrosine phosphorylation state of p130Cas by cortactin. Unphosphorylated p130Cas is mainly expressed in the cytoplasm as shown in Fig. 5B, whereas localization of p130Cas in the focal adhesion is thought to be required for tyrosine phosphorylation of p130Cas (28, 29). The results of immunocytostaining indicate that tyrosine-phosphorylated cortactin predominantly exists in the focal adhesion, and thus purging p130Cas from focal adhesion to lose the chance of being phosphorylated. Therefore, knockdown of cortactin might give chance for p130Cas to localize at the focal adhesion to be phosphorylated (Fig. 5). p130Cas was originally found as a prominent substrate of SFKs, including c-Src and Fyn during the transformation of cells (21, 30). It has been shown that phosphorylated p130Cas in focal adhesion plays a regulatory role in cell spreading and cell migration (19, 31-33), and knockdown of p130Cas actually abrogated cell migration in our gastric cancer cells, HSC44PE, even in the absence of cortactin (Fig. 3A and B). These results indicate that activation of p130Cas-mediated signal might be responsible for the enhancement of cell motility in the cells where hyperphosphorylated cortactin is knocked down.

Our study sheds new light on the cross-talk between cortactin and p130Cas, both of which are Src substrates. Such cross-regulation between SFK substrates might give more optimized outcome out of overlapping or conflicting effects of SFK signals. However, there is still a possibility that phosphorylated cortactin may also transduce specific signals regulating cell migration, which is independent of a function of p130Cas. As far as we examined, there was no significant effect on the morphology, cell-matrix adhesion, or number of focal adhesions in HSC44PE cells by suppression of cortactin expression (Fig. 5A and data not shown). On the other hand, it has been suggested that cortactins originally support cell migration through several pathways and therefore its tyrosine phosphorylation may have an inhibitory effect on these pathways. Binding of cortactin with N-WASP via its SH3 domain may synergize in causing actin polymerization

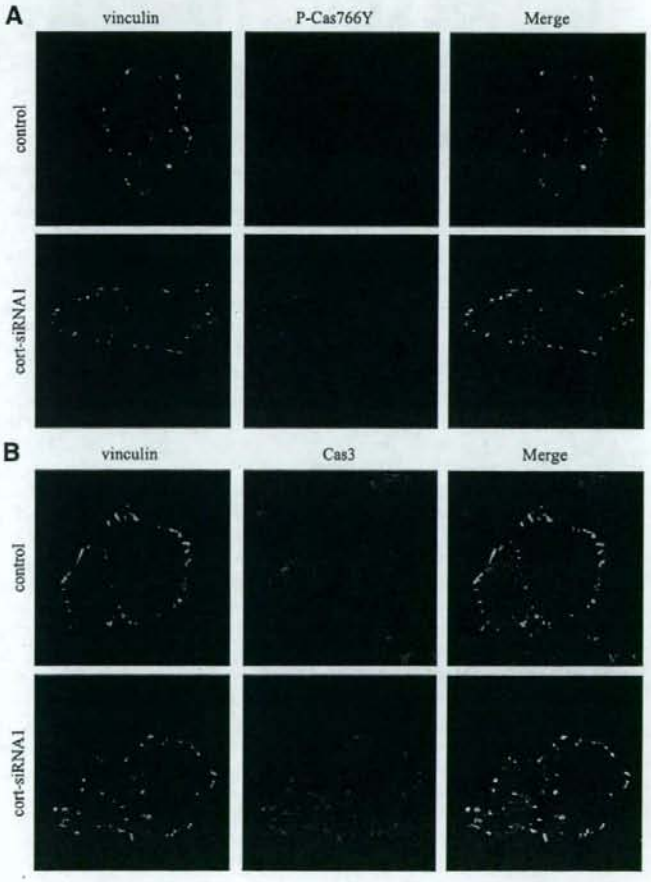

FIGURE 5. Changes in localization of p130Cas by treatment with cortactin siRNA. **A.** HSC44PE cells were transfected with cortactin siRNA or control siRNA for 72 h before localization of phosphorylated p130Cas was analyzed by immunocytostaining with P-Cas766Y antibody. Anti-vinculin antibody was used to visualize focal adhesions. Merged images indicate that tyrosine-phosphorylated p130Cas, which was greatly increased by cortactin siRNA, specifically localizes at focal adhesion. **B.** In HSC44PE cells treated with control or cortactin siRNA, localization of p130Cas was analyzed by anti-Cas3 antibody. A portion of p130Cas shows distinct colocalization with vinculin at focal adhesion in cells treated with cortactin siRNA, whereas staining of vinculin and p130Cas did not significantly overlapped in cells treated with control siRNA.

preceding cell migration, which is promoted by a serine kinase Erk and conversely inhibited by Src kinase (34). We showed all these signal pathways of phosphorylated cortactin in a schema (Fig. 6). In summary, tyrosine phosphorylation of cortactin might act as a unique and naïve switch in the regulation of cell motility. Our study offers new insight into cortactin for understanding its biological function in cancer progression.

Materials and Methods

Cell Culture

Human breast cancer cell line MCF7 was maintained in DMEM containing 10% (v/v) fetal bovine serum (Life Technologies) and 50 μg/mL penicillin-streptomycin antibiotics. Human gastric cancer cell lines HSC57, HSC44As3, HSC44PE, and HSC58As9 was supplied by Central Animal Laboratory, National Cancer Center Institute, Tokyo, Japan (24). They were maintained in RPMI 1640 supplemented with 10% fetal bovine serum and antibiotics.

Antibodies and Reagents

Anti-phosphotyrosine (4G10) and anti-cortactin (clone 4F11) antibodies were obtained from Upstate Biotechnology. Polyclonal antibodies Fyn3 and anti-FAK were purchased from Santa Cruz Biotechnology. Anti-paxillin and anti-green fluorescent protein (GFP) antibodies were purchased from Zymed and MBL, respectively. Anti-phospho-paxillin (Tyr^{118}), anti-phospho-FAK (Tyr^{397}), and anti-phospho-cortactin (Tyr^{421}) antibodies were purchased from Cell Signaling Technology, Upstate Biotechnology, and Chemicon, respectively. Anti-Flag-M2 antibody was obtained from Sigma. Polyclonal antibodies against p130Cas (Cas2 and Cas3) and phosphospecific polyclonal antibody P-Cas460Y were used as described previously (30, 35). Another phosphospecific antibody, P-Cas766Y, was generated by immunizing rabbits with a synthetic phosphopeptide, CMEDpYDpYVHL, which includes the phosphotyrosine-containing motifs in the Src-binding domain of p130Cas, after being conjugated with thymoglobulin. As secondary antibodies, horseradish peroxidase–conjugated anti-rabbit and anti-mouse IgG (Amersham) were used. Polylysine, fibronectin, and cycloheximide were purchased from Sigma. Inhibitor of SFKs, 4-amino-5-(4-chlorophenyl)-7-(*t*-butyl) pyrazolo [3,4-*d*] pyrimidine (PP2), and the inactive structural analogue 4-amino-7-phenylpyrazol [3,4-*d*] pyrimidine (PP3) were obtained from Calbiochem-Novabiochem Ltd.

RNA Interference Experiments for Cortactin and p130Cas

Two independent siRNA of human cortactin, cort-siRNA1 and cort-siRNA2, for RNA interference experiment were generated by Invitrogen Life Technologies. Cort-siRNA1 targets cortactin mRNA at 5′-CCCAGAAAGACUAUGUGAAAGG-GUU-3′ and Cort-siRNA2 targets at 5′-GGAGAAGCACGA-GUCACAGAGAGAU-3′. The siRNA of human p130Cas was also generated by Invitrogen Life Technologies, using the target sequence 5′-CCAAGAUCUUUGUGGCGCACAGCAA-3′. For transient transfection of siRNA, the cells were plated at 1.5×10^5 per well on a six-well plate. Transfection of siRNAs was done with Lipofectamine 2000 (Invitrogen Co.). After transfection for 72 h, the cells were harvested for the biochemical analyses.

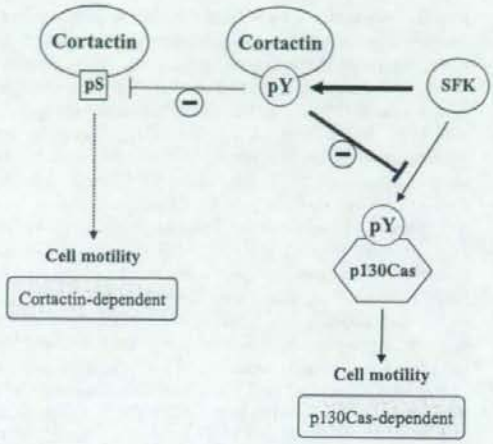

FIGURE 6. Schematic view of multiple roles of cortactin in the regulation of cancer cell motility.

Infection of Retroviral Constructs

Retrovirus vectors were used to express mouse cortactin fused with GFP (pjl6) and F421F466F482 triple mutant of mouse cortactin fused with GFP (pJL12; ref. 4). Briefly, the retroviral vector and the packaging construct pCL-10A1 were cotransfected into 293T cells and culture fluid was harvested 72 h posttransfection. HSC44PE cells were infected with the viral fluid in the presence of 4 mg/mL polybrene, and the infected cells were selected in the presence of 800 μg/mL Geneticin G418 (Sigma) for a period of 2 to 3 wk.

Establishment of Stable MCF7 Clones Expressing Fyn Kinase

Breast cancer cells MCF7 were grown in DMEM containing 10% fetal bovine serum and antibiotics. On the night before transfection, the cells were seeded onto a 10-cm dish at a density of 9.0×10^5. Transfection of a vector expressing Fyn kinase with a tag of Flag (Fyn-Flag) and an original vector (pcDNA3.1) was done according to the manufacturer's instructions. Twenty-four hours after transfection, the cells were subjected to selection by Geneticin G418 (Sigma) at a concentration of 800 μg/mL for a period of 2 to 3 wk.

Immunoblotting and Immunoprecipitation

For immunochemical analysis, cells were cultured in the incubator at 37°C with 5% CO_2 for 48 to 72 h, before the cells were lysed in 1% Triton X-100 buffer (50 mmol/L HEPES, 150 mmol/L NaCl, 10% glycerol, 1% Triton X-100, 1.5 mmol/L $MgCl_2$, 1 mmol/L EGTA, 100 mmol/L NaF, 1 mmol/L Na_3VO_4, 10 μg/mL aprotinin, 10 μg/mL leupeptin, 1 mmol/L phenylmethylsulfonyl fluoride), and insoluble material was removed by centrifugation for 10 min. Protein concentration was analyzed by BCA Protein Assay (Pierce), and the protein

aliquots were separated by SDS-PAGE. Gels were transferred to the polyvinylidene difluoride membrane (Millipore) and subjected to immunoblotting. After blocking with 5% skim milk in TBST [100 mmol/L Tris-HCl (pH 8.0), 150 mmol/L NaCl, and 0.05% Tween 20] for 1 h, blots were incubated with primary antibodies. In the case of 4G10, blocking was done with Blocking One Solution (Nakarai Co.). Membranes were then washed thrice with TBST, incubated with horseradish peroxidase–conjugated secondary antibodies for 30 min at room temperature, washed thrice by TBST again and once by TBS [100 mmol/L Tris-HCl (pH 8.0), 150 mmol/L NaCl], and visualized by autoradiography using a chemiluminescence reagent (Western Lighting, Perkin-Elmer).

For immunoprecipitation, 500 μg of protein were mixed with 2 μg of antibodies and incubated for 1 h on ice, and then samples were rotated with protein G–Sepharose beads (Amersham Pharmacia) for 2 h at 4°C. The beads were washed thrice with 1% Triton X-100 buffer and boiled in sample buffer [2% SDS, 0.1 mol/L Tris-HCl (pH 6.8), 10% glycerol, 0.01% bromphenol blue, 0.1M DTT] for SDS-PAGE analysis.

Immunocytostaining

Approximately 5×10^4 cells were plated on 12-mm circle cover glasses on a 24-well plate, which were grown in DMEM with 10% fetal bovine serum at 37°C with 5% CO_2 for 24 h. The 12-mm circle cover glasses were coated by fibronectin 10 μg/mL in PBS overnight before seeding the cells. Then, cells were fixed in 4% paraformaldehyde in 0.1 mol/L sodium phosphate (pH 7.0) for 5 min, washed thrice with PBS, and permeabilized with 0.1% Triton X-PBS for 10 min before blocking with 5% bovine serum albumin with TBST [0.15 mol/L NaCl, 1% Tris (pH 7.0), 0.05% Tween 20] for 10 min. Then, the cells were incubated with the first antibody for 1 h at room temperature. Cells were washed with PBS thrice, and incubated with appropriate second Alexa antibodies (Molecular Probe; 1:500) in 5% goat serum with 3% bovine serum albumin/TBST. All cover glasses were mounted in 1.25% DABCO, 50% PBS, and 50% glycerol. The staining was visualized using a Radiance 2100 confocal microscopic system (Bio-Rad).

Cell Migration Assay

Migration assay was done using modified Transwell chambers with polycarbonate Nucleopore membrane (Falcon, BD). Precoated filters (6.5 mm in diameter, 8-μm pore size, fibronectin 10 μg/mL) were rehydrated with 100 μL medium. Then, 4×10^4 cells in 100 μL serum-free DMEM supplement were seeded onto the upper part of each chamber, whereas the lower compartments were filled with 600 μL of the same medium with 10% fetal bovine serum. Following incubation for 8 h at 37°C, nonmigrated cells on the upper surface of the filter were wiped out with a cotton swab, and the migrated cells on the lower surface of the filter were fixed and stained with Giemsa stain solution (Azur-Eosin-Methylene Blue Solution, Muto Pure Chemicals, Co., Japan). The total number of migrated cells was determined by counting cells in five microscopic fields per well at a magnification of ×100, and the extent of migration was expressed as the average number of the cells per microscopic field.

Acknowledgments

We thank Dr. Xi Zhan for mouse cortactin constructs and Dr. Hitoyasu Futami for critical reading of the manuscript.

References

1. Schuuring E, Verhoeven E, Litvinov S, Michalides RJ. The product of the EMS1 gene, amplified and overexpressed in human carcinoma, is homologous to a v-src substrate and is located in cell-substratum contact sites. Mol Cell Biol 1993;13:2891–8.

2. Campbell DH, deFazio A, Sutherland RL, Daly RJ. Expression and tyrosine phosphorylation of EMS1 in human breast cancer cell line. Int J Cancer 1996;68: 485–92.

3. Hui R, Ball JR, Macmillan RD, et al. EMS1 gene expression in primary breast cancer relationship to cyclin D1 and oestrogen receptor expression and patient survival. Oncogene 1998;17:1053–9.

4. Li Y, Tondravi M, Liu J, et al. Cortactin potentates bone metastasis of breast cancer cells. Cancer Res 2001;61:6906–11.

5. Patel AM, Incognito LS, Schechter GL, Wasilenko WJ, Somers KD. Amplification and expression of EMS-1 (cortactin) in head and neck squamous cell carcinoma cell lines. Oncogene 1996;12:31–5.

6. Freier K, Sticht C, Hofele C, et al. Recurrent coamplification of cytoskeleton-associated genes EMS1 and SHANK2 with CCND1 in oral squamous cell carcinoma. Genes Chromosomes Cancer 2006;45:118–25.

7. Daly RJ. Cortactin signaling and dynamic actin networks. Biochem J 2004; 382:13–25.

8. Lua BL, Low BC. BPGAP1 interacts with cortactin and facilitates its translocation to cell periphery for enhanced cell migration. Mol Biol Cell 2004; 15:2873–83.

9. Du Y, Weed SA, Xiong WC, Marshall TD, Parsons JT. Identification of a novel cortactin SH3 domain-binding protein and its localization to growth cones of cultured neurons. Mol Cell Biol 1998;18:5838–51.

10. Kowalski JR, Egile C, Gil S, Snapper SB, Li R, Thomas SM. Cortactin regulates cell migration through activation of N-WASP. J Cell Sci 2005;118: 79–87.

11. Wu H, Parsons JT. Cortactin, an 80/85-kilodalton pp60src substrate, is a filamentous actin-binding protein enriched in the cell cortex. J Cell Biol 1993; 120:1417–26.

12. Kim L, Wong TW. Growth factor-dependent phosphorylation of the actin-binding protein cortactin is mediated by the cytoplasmic tyrosine kinase FER. J Biol Chem 1998;273:23542–8.

13. Gallet C, Rosa JP, Habib A, Lebret M, Levy-Toledano S Maclouf J. Tyrosine phosphorylation of cortactin associated with Syk accompanies thromoxane analogue-induced platelet shape change. J Biol Chem 1999;274: 23610–6.

14. Campbell DH, Sutherland RL, Daly RJ. Signaling pathways and structural domains required for phosphorylation of EMS1/cortactin. Cancer Res 1999;59: 5376–85.

15. Vidal CB, Geny J, Melle M, Jandrot-Perrus M, Fontenay-Roupie. Cdc42/Rac1-dependent activation of the p21-activated kinase (PAK) regulates human platelet lamellipodia spreading implication of the cortical-actin binding protein cortactin. Blood 2002;100:4462–9.

16. Huang J, Asawa T, Takato T Sakai R. Cooperative roles of Fyn and cortactin in cell migration of metastatic murine melanoma. J Biol Chem 2003; 278:48367–76.

17. Webb DJ, Parsons JT, Horwitz AF. Adhesion assembly, disassembly and turnover in migrating cells—over and over and over again. Nat Cell Biol 2002;4: 97–100.

18. Mitchison TJ, Cramer LP. Actin-base cell motility and cell locomotion. Cell 1996;84:371–9.

19. Honda H, Oda H, Nakamoto T, et al. Cardiovascular anomaly, impaired actin bundling and resistance to Src-induced transformation in mice lacking p130Cas. Nat Genet 1998;19:361–5.

20. Huang J, Hamasaki H, Nakamoto T, et al. Differential regulation of cell migration, actin stress fiber organization, and cell transformation by functional domains of Crk-associated substrate. J Biol Chem 2002;277:27265–72.

21. Sakai R, Nakamoto T, Ozawa K, Aizawa S, Hirai H. Characterization of the kinase activity essential for tyrosine phosphorylation of p130Cas in fibroblasts. Oncogene 1997;14:1419–26.

22. Yanagihara K, Tanaka H, Takigahira M, et al. Establishment of two cell lines from human gastric scirrhous carcinoma that possess the potential to metastasize spontaneously in nude mice. Cancer Sci 2004;95:575–82.

23. Zhang LH, Tian B, Diao LR, et al. Dominant expression of 85-kDa form of cortactin in colorectal cancer. J Cancer Res Clin Oncol 2006;132:113–20.

24. Chuma M, Sakamoto M, Yasuda J, et al. Overexpression of cortactin is involved in motility and metastasis of hepatocellular carcinoma. J Hepatol 2004; 41:629–36.

25. Rothschild BL, Shim AH, Ammer AG, et al. Cortactin overexpression regulates actin-related protein 2/3 complex activity, motility, and invasion in carcinomas with chromosome 11q13 amplification. Cancer Res 2006;66: 8017–25.

26. Barroso C, Rodenbusch SE, Welch MD, Drubin DG. A role for cortactin in *Listeria monocytogenes* invasion of NIH 3T3 cells, but not in its intracellular motility. Cell Motil Cytoskeleton 2006;63:231–43.

27. Nakamoto T, Sakai R, Honda H, et al. Requirements for localization of p130cas to focal adhesions. Mol Cell Biol 1997;17:3884–97.

28. Huang C, Liu J, Haudenschild CC, Zhan X. The role of tyrosine phosphorylation of cortactin in the locomotion of endothelial cells. J Biol Chem 1998;273:25770–6.

29. Sawada Y, Tamada M, Dubin-Thaler BJ, et al. Force sensing by mechanical extension of the Src family kinase substrate p130Cas. Cell 2006; 127:1015–26.

30. Sakai R, Iwamatsu A, Hirano N, et al. A novel signaling molecule, p130, forms stable complexes *in vivo* with v-Crk and v-Src in a tyrosine phosphorylation-dependent manner. EMBO J 1994;13:3748–56.

31. Klemke RL, Leng J, Molander R, Brooks PC, Vuori K, Cheresh DA. CAS/Crk coupling serves as a "molecular switch" for induction of cell migration. J Cell Biol 1998;140:961–72.

32. Panetti TS. Tyrosine phosphorylation of paxillin, FAK and p130CAS: effects on cell spreading and migration. Front Biosci 2002;7:143–50.

33. Pratt SJ, Epple H, Ward M, Feng Y, Braga VM, Longmore GD. The LIM protein Ajuba influences p130Cas localization and Rac1 activity during cell migration. J Cell Biol 2005;168:813–24.

34. Martinez-Quiles N, Ho HY, Kirschner MW, Ramesh N, Geha RS. Erk/Src phosphorylation of cortactin acts as a switch on-switch off mechanism that controls its ability to activate N-WASP. Mol Cell Biol 2004;24:5269–80.

35. Miyake I, Hakomori Y, Misu Y, et al. Domain-specific function of ShcC docking protein in neuroblastoma cells. Oncogene 2005;24:3206–15.